Draft version March 30, 2017
Typeset using LaTeX **twocolumn** style in AASTeX61

THE VULTURE SURVEY II: ANALYZING THE EVOLUTION OF CIV ABSORBERS

Nigel L. Mathes, Christopher W. Churchill[1] and Michael T. Murphy[2]

[1] *New Mexico State University, Las Cruces, NM 88003*
[2] *Centre for Astrophysics and Supercomputing, Swinburne University of Technology, Victoria 3122, Australia*

ABSTRACT

We present things based upon CIV. We compare to MgII. Trends exist. Things are interesting.

Keywords: galaxies: halos — quasars: absorption lines

1. INTRODUCTION

One of the most elusive yet important goals in extragalactic research aims to discover how galaxies form, grow, and evolve in an effort to truly understand our place in the universe. The creation of a galaxy begins with a cosmic overdensity, where matter congregates to begin the process of building complex structures of stars, gas, and dust. Feedback from star formation and AGN, along with mergers, shape the galaxy and its surroundings into complex environments. The stage of most uncertainty throughout this process involves feedback, the injection of energy into the gaseous medium within and outside of galaxies which, as has been shown in simulations, is required to produce realistic looking galaxies.

The details of this complex process should be observable in the relationship between the stars in the galaxy and the gas phase material located between the stars within the galaxy (interstellar medium; ISM), just outside the galaxy (circumgalactic medium; CGM), and between galaxies themselves (intergalactic medium; IGM). Unfortunately, detailed observations of this gas are difficult as it remains mostly neutral (CITATION), and therefore does not strongly emit. Therefore, massive efforts have been undertaken to observe this gas in absorption using the most advanced telescopes.

CIV absorption lines are some of the better tracers of metal enriched gas around galaxies across cosmic time due to their existence in a wide range of astrophysical conditions, and their ease of observation with optical, ground-based telescopes. Specifically, the CIV $\lambda\lambda 1548, 1550$ doublet traces gas around galaxies with ionization parameters from $SOMETHING < \log U < SOMETHINGELSE$, and from redshifts $1 < z < 5$ in optical spectra. These absorbers have high oscillator strengths and trace an abundant metal, allowing for detections even in low metallicity gas with sufficiently high signal-to-noise spectra, making them ideal for inventorying a large portion of the CGM and IGM.

Beginning history of things here:

The first study to characterize intervening CIV absorbers was /citeYoung1982, which determined that these lines were randomly distributed in redshift in a manner consistent with absorption from intervening galaxies. /citeSargent1988 also showed that the number density of systems per unit redshift decreases with increasing redshift from $1.8/lez_{em}/le3.56$. /citeSteidel1990, examining strong CIV absorbers at redshifts between $1.3/lez_{abs}/le4.0$, found also that the number of CIV absorption systems per unit redshift range decreases with increasing redshift, in a manner inconsistent with a constant comoving density of absorbers. Therefore, they stated, the properties of CIV absorbers must evolve over time.

In terms of kinematics, /citeSteidel1990 noted that the peak in the CIV two-point correlation function on velocity scales $200/le\Delta v/le600$ km s^{-1} appears to have the same power at low and high redshift. /citeRauch1996 examined the velocity structure of intervening CIV absorbers in the spectra of 3 intermediate redshift quasars and detrmined that gas temperatures were likely near $3.8/times10^4$ $/mathrmk$, and the TPCF of CIV systems suggests that there is more than one source of velocity dispersion. They interpret the shape of the resulting TPCF as owing to ensembles of objects with the kinematics of dwarf galaxies on a small scale, while following the Hubble flow on a larger scale.

? examined data from the Hubble Space Telescope Faint Object Spectrograph for CIV absorbers associated with known MgII absorbers measured in high resolution Keck/HIRES data. They noticed a strong correlation between MgII kinematics and CIV equivalent width. They interpreted that this correlation could imply a connection between outflowing MgII clouds and higher ionization state halo gas.

? measured the kinematics and column density differences of CIV absorption systems along the lines of sight to three gravitationally lensed quasars. They found the spatial distribution of the gas to be mostly featureless with detectable velocity shear up to $\sim$ 70 kms. They found the clouds quiescent, in that the energy transmitted to the gas as measured by the amount of turbulence derived along the line of sight, and therefore determined that the absorbing structures are not internal to galaxies. They posited that CIV absorbers could be gas expelled recently or pre-enriched from earlier star formation.

? examined 14 galaxy absorber pairs, along with 36 galaxies without associated CIV absorption lines. They found that CIV absorption line systems cluster strongly on velocity scales of $v \lesssim 250$ km s^{-1} and impact parameter scales of $\rho \lesssim 100$ h^{-1} kpc. In addition, they note that galaxies of all morphological types and luminosities can possess extended gaseous envelopes, with covering factors near unity, at impact parameters less than 100 kpc. They concluded that accreting satellites are the most likely sources of this metal enriched halo gas.

?, **?**, and **?** all measured the comoving number of CIV absorbers per redshift path length in the spectra of background quasars. Together, they find that, when considering CIV absorbers with equivalent widths greater than $W_r^{1548} > 0.3$ Å, the number of absorption doublets

per unit redshift decreases with increasing redshift for $1.2 < z < 4.5$.

? directly measured the metallicity distribution function for the $z \sim 2.5$ intergalactic medium in the spectra of seven quasars. They found no evidence for a universal metallicity floor, as had been suggested for some scenarios of Population III enrichment in the early universe. In addition, they found no trends in metallicity as a function of IGM density.

? used a novel method of identifying pseudoclouds in C IV $\lambda\lambda 1548, 1550$ systems and measuring their individual properties with the pixel optical depth method. She generated the C IV column density distribution, and calculated from it the cosmic mass density of C IV absorbers ($\Omega_{\rm C\,IV}$) from $2 < z < 5$. She found a lack of redshift evolution in ($\Omega_{\rm C\,IV}$) for absorbers of all column densities, with ($\Omega_{\rm C\,IV}$) $\simeq 5\times10^{-8}$ at $z = 2$ and ($\Omega_{\rm C\,IV}$) $\simeq 2\times10^{-8}$ at $z = 5$.

In the following paper in this series, **?** attempted to identify C IV systems associated with galactic outflows. By analzying velocity widths, she found that roughly half of the systems with τ(C IV) > 0.4 have widths consistent with outflowing winds. She concluded, after accounting for ionization from galaxy-like spectra and AGN, that almost all lower column density systems and roughly half of high column density C IV systems lie in the iGM, while half of the highest column density systems could be the direct result of outflows ionized by their parent galaxies.

? analyzed a single high equivalent width C IV system at $z_{abs} = 5.7238$, reporting that neither the column density distribution nor its integral evolves significantly from 1 to 4.5 Gyr after the big bang. This high redshift detection imples that either a large fraction if intergalactic metals were in place even at high redshift, or that this high column density system has origins in a highly ionized outflow.

? studied 63 damped Lyman-α (DLA) systems and 11 sub-DLAs with associated C IV absorption. They detected C IV clouds moving at velocites in excess of the escape speed, determined by measuring the total line width of the neutral gas profile, in roughly 40% of their systems. They inferred that these clouds may arise in high ionized outflowing winds, powered by galaxies with star formation rates (SFR) of $\sim 2\ M_\odot\ {\rm yr}^{-1}$.

? surveyed 49 low redshift quasars with high resolution *Hubble Space Telescope* ultraviolet (UV) spectra for $z < 1$ C IV candidates. They were able to measure dN/dX, finding that it has not significantly evolved since $z = 5$. They also constructed the column density frequency distribution, fitting it with a power law of exponent of $\alpha = -1.50$. Finally, they calculated $\Omega_{\rm C\,IV}$, finding a value roughly 3 times higher than at $z \sim 5$, showing that the cosmic mass density of C IV has slowly but steadily increases from $z = 5$ to $z = 0$.

? measured the intergalactic C IV mass density at $4.3 < z < 6.3$ using the Magellan Folded-Port Infrared Echellette (FIRE) spectrograph. They confirmed the downturn in $\Omega_{\rm C\,IV}$ at $z > 4$. They postulated that, due to the short physical timescaled at these redshifts, this downturn may be driven primarily by ionization conditions. However, they cautioned that low number statistics still pose problems due to the limited number of sightlines to high redshift quasars.

? used the Sloan Digital Sky Survey (SDSS) Data-Release 7 (DR7) to survey over 16,000 C IV systems with $1.46 < z < 4.55$ and rest frame equivalent widths ($W_r^{\lambda1548}$) greater than 0.3 Å. They found that the equivalent width frequency distribution ($f(W_r)$) was well-modelled by an exponential, with little evolution in its shape. In addition, they found dN/dX increased smoothly with decreasing redshift from $z = 4.55$ to $z = 1.96$ before plateauing at redshifts below 1.96. Their results suggest a monotonic increase in the amount of C IV enriched gas outside galaxies over the history of the universe.

? used *HST*/COS spectra of background quasars to measure elemental abundances in the low redshift intergalactic medium. They found that C IV has increased in abundance by a factor of 10 from $z \sim 5$ to present.

? measured C IV absorption in the COS-Dwarfs survey, probing the gaseous halos near 43 low-mass galaxies at $z \geq 0.1$. They detected C IV out to ~ 100 kpc, roughly $0.5R_{vir}$, from the host galaxies. They also reported a tentative correlation between C IV equivalent width and SFR, and concluded that energy-driven star formation winds must expel into the CGM a comparable mass to that of the carbon found in the stars of these galaxies.

? conducted a blind search of 89 quasar sightlines observed with the *HST* Cosmic Origins Spectrograph (COS) for low redshift C IV absorption. They identified 42 absorbers with $z < 0.16$. They determined that the number density of C IV abosrbers per comoving path length and cosmic mass density relative to the critical density both increase marginally from $z \sim 1.5$ to present, confirming both extrapolated trends from higher redshifts and predictions from cosmological hydrodynamic simulations.

We begin by explaining the methods of acquiring and analyzing the quasar spectra in section 2. Next, in section 3, we present the results showing the evolution of the C IV equivalent width distribution, dN/dX, and the C IV column density distribution across redshift. In

section 4 we analyze the funcitonal fit to the column density distribution and derive the relative matter density contributed to the universe by CIV, $\Omega_{\rm CIV}$. We also compare CIV to MgII in hopes of uncovering any global trends with metals in galaxy halos across redshifts spanning $0.1 < z < 5$. In Section 5 we summarize our results and look to future studies using this rich data set, including a companion analysis of intervening CIV absorbers and detailed kinematic analysis of intervening absorbing systems. For all calculations, we adopt the most recently published Planck cosmology, with $H_0 = 67.74$ kms^{-1}Mpc, $\Omega_M = 0.258$, and $\Omega_\Lambda = 0.742$.

2. DATA AND ANALYSIS

2.1. *Sample and Analysis*

The Vulture survey makes use of archival VLT/UVES and KECK/HIRES quasar spectra compiled by the UVES Squad group, led by Michael T. Murphy, and the KODIAQ collaboration, described in O'Meara et al. (2015). The spectra range in signal-to-noise from 4 to 288, quasar emission redshifts span $0.014 < z < 5.292$, and wavelength coverage for each spectrum spans either $3000-6600$ Å or $3000-10,000$ Å, depending upon whether the red arm of each spectrograph was used.

The data are continuum normalized, inspected, and then fed into automated line detection software to find all CIV $\lambda\lambda1548, 1550$ systems through a matched filtering technique. Equivalent width detection limits are calculated through a self-monitoring technique which evaluates the detection sensitivity for each spectrum as a function of wavelength. Then, the detections are visually verified, and any absorption systems within ±500 km s^{-1} are combined into one system for analysis. These processes are described in detail in **?**.

Within the absorbing regions, we calculate equivalent widths (W_r), velocity widths (Δv), kinematic spreads (ω_v), and apparent optical depth (AOD) column densities ($log(N)$).

3. RESULTS

3.1. *Sample Characterization*

Figure 1 shows the relationships between the measured absorption parameters, characterizing the distribution of absorption properties for our survey. We cover a large parameter space, examining all types of observable absorption systems from $< W_r^{\lambda1548} < 5$ Å

3.2. *Sample Completeness and Survey Path Coverage*

Figure 2 shows the function $g(W_r^{1548}, z)$. This 2D heat map details the number of spectra in which a CIV $\lambda\lambda1548, 1550$ doublet could be detected as a function of the equivalent width detection limit and redshift. The vertical stripes with no redshift path coverage represent the omitted telluric absorption regions for our survey. The integral along a given W_r^{1548} slice gives the total redshift path length available for the sample.

3.3. *dN/dZ and dN/dX*

Previous studies of the statistical properties of CIV absorbers have thoroughly characterized CIV absorbers with equivalent widths above $W_r^{\lambda1548} = 0.3$ Å. This corresponds to the detection limit of the Sloan Digital Sky Survey (SDSS), which catalogs hundreds of thousands of quasar spectra. Unfortunately, the distribution of the low equivalent width regime of CIV absorbers has not been characterized.

We follow the prescriptions of Paper 1, in which we details the calculations of dN/dz and dN/dX, the redshift path density and absorption path density, respectively. These metrics describe the expected number of detected absorbers through a given redshift or absorption path length.

In Figures 3 and 4, we plot dN/dz and dN/dX as a function of redshift for varying equivalent width cuts. Dotted lines are fit according to the analytical form which allows for redshift evolution in dN/dX, defined as,

$$\frac{dN}{d(z,X)} = n\sigma(1+z)^\epsilon, \tag{1}$$

where n is the number density of CIV absorbers, σ is the absorbing cross-section, and ϵ is the power dependence of dN/dX on redshift. As we apply larger equivalent width cuts, $n\sigma$ decreases, representing a decreasing incidence of very strong CIV absorbers, whether by decreasing number density, absorbing cross-section, or both. In addition, ϵ becomes more negative with increasing equivalent width cuts up until around $W_r^{\lambda1548} = 1$ Å, at which point it tends toward 0. This transition at $W_r^{\lambda1548} = 1$ Å occurs not because the overall slope of the distribution necessarily changes, but instead because the distribution takes on SOME SHAPE, where dN/dz and dN/dX peak around $z = 2$, but decrease towards higher and lower redshifts.

Talk about Figure 5 and 6.

3.4. *Equivalent Width Frequency Distribution*

We calculate the equivalent width frequency distribution by first calculating dN/dz and dN/dX for each absorber equivalent width, then summing the distribution in equivalent width bins, and then dividing by the bin width. We examine four redshift bins, requiring that

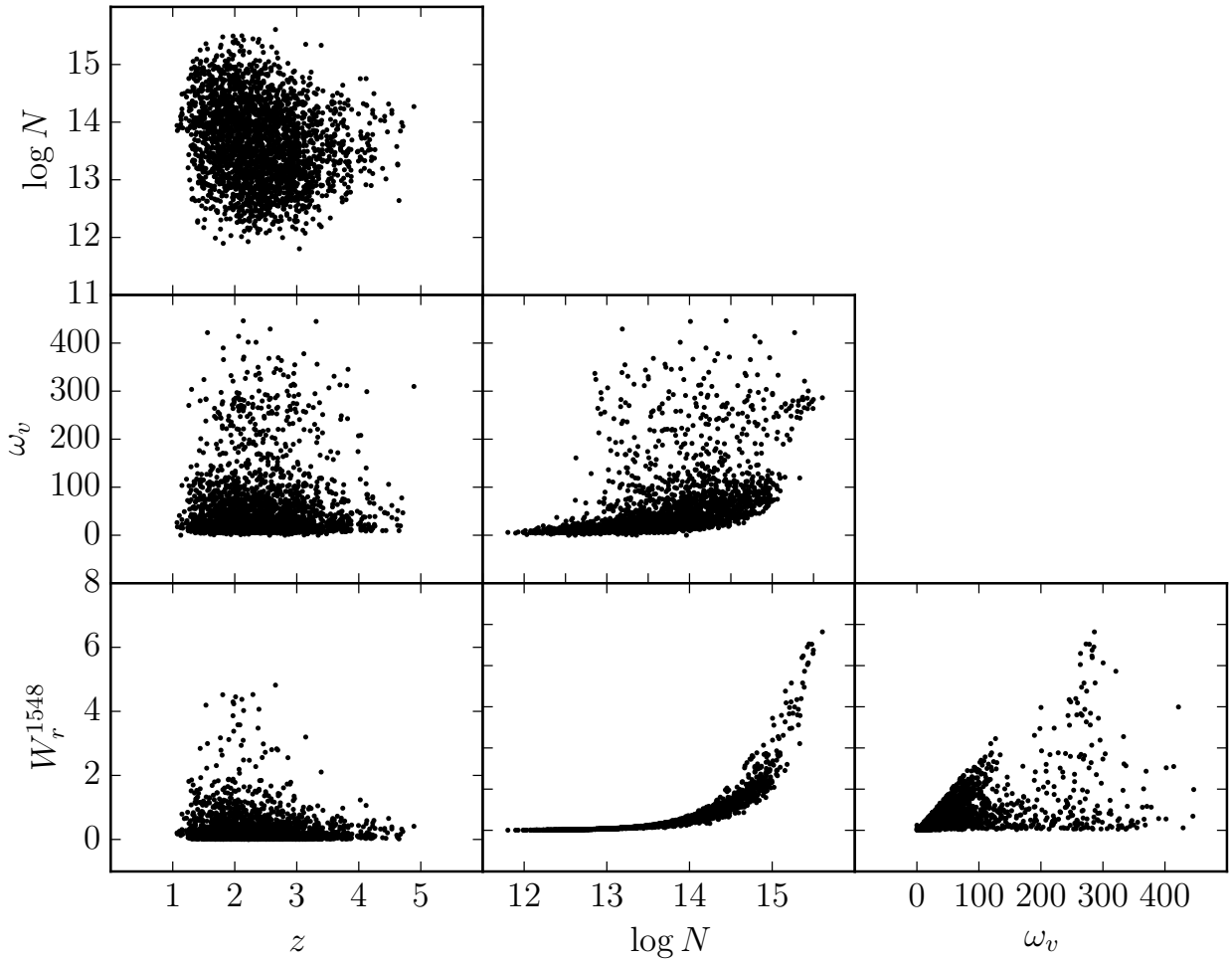

Figure 1. Correlations between measured absorption properties for survey sample. $\log N$ is the AOD column density, ω_v is the kinematic spread, W_r^{1548} is the rest frame CIV1548 equivalent width, and z is the absorption redshift.

the number of absorbers in each redshift range remains constant.

In Figure 8, we plot the equivalent width frequency distribution. We fit this distribution with a Shechter function to parameterize the distribution and to compare the relative differences between varying redshift cuts. We find the low equivalent width slope decreases towards shallower values as redshift increases, implying a decrease in weak CIV absorbers and a relative increase in strong CIV absorbers from low redshift to redshifts near $z = 2$.

3.5. *Column Density Distribution*

To calculate the column density distribution, we calculate $dN\,/dX$ for each absorber equivalent width, sum the distribution in column density bins, and then divide by the bin width. The result is a characteristic number density of CIV absorbers per absorption path length as a function of their column densities. It should be noted that at high column densities near $\log(N(CIV)) = 15$, the measured column densities are lower limits as the AOD method to measure column densities cannot constrain the true column when the line saturates.

In Figure 10, we plot the column density frequency distribution. Again, we fit this distribution with a Schechter function. We find again that the low column density end of the distribution becomes shallower as one goes from low redshift to $z = 2$. Due to saturation effects, the final high column density bin is likely best regarded as a lower limit.

3.6. *Comparison with* MgII *Absorption Properties*

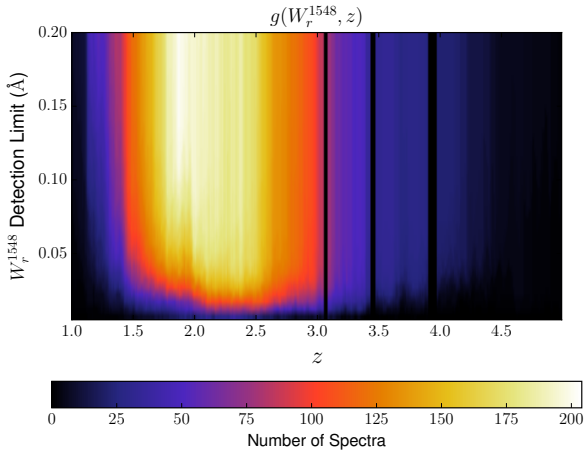

Figure 2. The function $g(W_r^{1548}, z)$ shown as 2D heat map with the colors representing the value of $g(W_r^{1548}, z)$. This is the number of spectra in which an absorption line of a given equivalent width and a given redshift may be detected according to the detection limit of the spectrum. The vertical black bars representing no redshift path length coverage show the omitted wavelength regions of the survey based upon contaminating telluric absorption features.

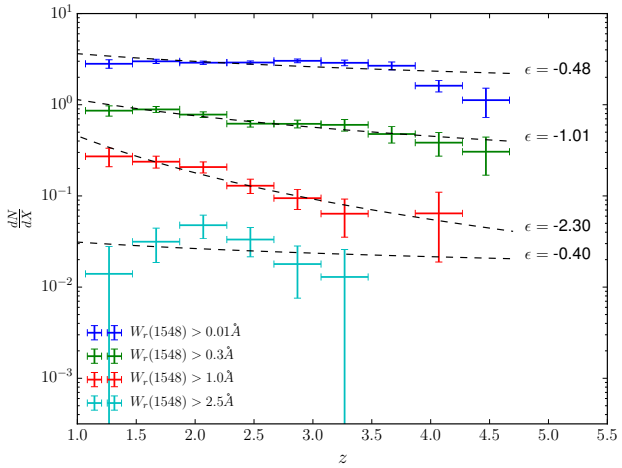

Figure 4. $\frac{dN}{dX}$ as a function of redshift for varying $W_r^{\lambda 1548}$ cuts. Colors represent different equivalent width cuts. The black dotted lines are fits to the distribution of the functional form $f(z) = n\sigma(1+z)^{\epsilon}$, with the best fit ϵ value labelled. We see increasing values of ϵ with increasing equivalent width, driven by an enhancement of stronger CIV absorbers around redshift 2 compared to lower redshifts.

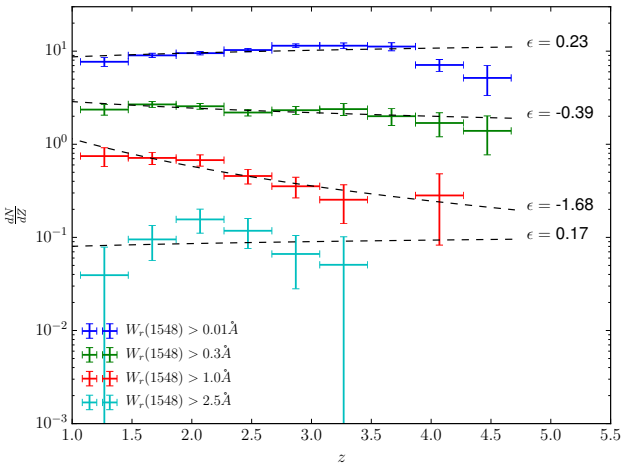

Figure 3. $\frac{dN}{dZ}$ as a function of redshift for varying $W_r^{\lambda 1548}$ cuts. Colors represent different equivalent width cuts. The black dotted lines are fits to the distribution of the functional form $f(z) = n\sigma(1+z)^{\epsilon}$, with the best fit ϵ value labelled.

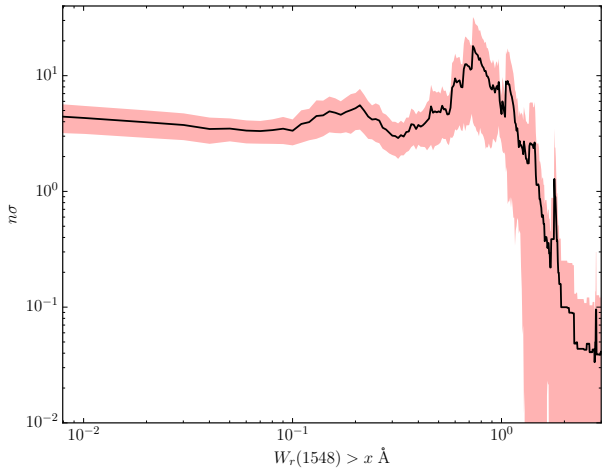

Figure 5. Absorber space density times cross section, as derived from the funtional fit $dN/dX = n\sigma(1+z)^{\epsilon}$ as a function of cumulative equivalent width cut, where $W_r^{\lambda 2796} > x$ Å. As CIV equivalent width increases, either the space density of absorbing cloud structures decreses, the absorbing cross-section decreases, or both parameters decrease.

Comparison plots and comparison table of evolution of Schechter fits and evolution of dN/dX plotted on the same axis.

4. DISCUSSION

4.1. *Evolution of CIV Distributions*

Discuss all previous CIV surveys in order.

Discuss Jane's interpretation of changing ionizing background in order to link the CIV and MgII properties.

4.2. $\Omega_{\rm CIV}$

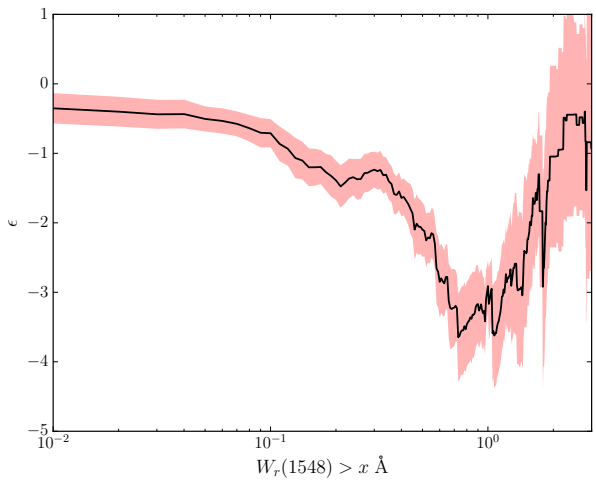

Figure 6. Redshift power dependence of the functional fit $dN/dX = n\sigma(1+z)^{\epsilon}$ as a function of cumulative equivalent width cut, where $W_r^{\lambda 2796} > x$ Å. Weak CIV absorbers are more abundant at low redshift, leading to a negative coefficient ϵ. Moderate equivalent width CIV absorbers do not evolve, showing $\epsilon \simeq 0$. Strong CIV absorbers evolve away at low redshift, showing a large positive ϵ increasing towards $z = 2$.

We now aim to calculate the matter density of CIV absorbers across cosmic time using the following equation,

$$\Omega_{CIV} = \frac{H_0\ m_{Mg}}{c\ \rho_{c,0}} \int_{N_{min}}^{N_{max}} f(N_{CIV})\, N_{CIV}\, dN_{CIV}, \quad (2)$$

where H_0 is the Hubble constant today, $m_{Mg} = 4.035 \times 10^{-23}$ g, c is the speed of light, $\rho_{c,0}$ is the critical density at present, $f(N_{CIV})$ is the column density distribution of CIV absorbers, and N_{CIV} is the column density. We numerically integrate the Schecter Function fit to $f(N_{CIV})$, multiplied by N_{CIV}. The results are shown below in Figure 11.

Errors are derived by bootstrap Monte-Carlo, performing the same sample analysis outlined in Sections 3.5 and 4.2 on a random sample, selected with replacement, of CIV absorbers. We take the standard deviation about the mean of this ensemble of random samples as the error in Ω_{CIV}.

4.3. *Potential Causes for Trends*

The most obvious conclusion to be drawn from our CIV survey is that around redshift $z = 2$, something changes in the distribution of CIV absorbers. The number of strong absorbers per unit path length increases, the faint end slope of the equivalent width and column density distributions flattens, the 'knee' of the Shechter fit of the equivalent width and column density distributions pushes outward to higher $W_r^{\lambda 1548}$ and N(CIV), and the cosmic mass density of CIV increases. We can now state that the physical properties driving the global distribution of CIV absorbers changes around $z = 2$. Possible explanations relate to the ionization conditions in the halos of galaxies at this time, the metallicity of gas around galaxies, or the quantity of metals in the circumgalactic medium.

Haardt & Madau (2012) represents the most recent and robust estimate of the cosmic ionizing background as a function of redshift, which is the primary ionizing component responsible for the global ionization state of gas in galactic halos. REDSHIFT EVOLUTION OF BACKGROUND RADIATION. DISCUSS HOW THIS DOES NOT PRODUCE TRENDS.

The metallicity of galaxy halos as a whole is not well characterized over time. However, if we assume that the metals in galaxy halos are built up as a result of outflows (Quiret et al. 2016), and that the metallicty of the halo may scale with the metallicity of the ISM, then it would make no sense to observe larger quantities of CIV in the circumgalactic medium at $z = 2$ compared to HIGHER REDSHIFTS. DISCUSS HOW THIS DOES/DOES NOT SUPPORT THE TRENDS WE OBSERVE.

5. CONCLUSIONS

Using archival data from VLT/UVES and $KECK$/HIRES, we have undertaken the most complete survey of CIV absorbers in 602 quasar spectra in high resolution (~ 7 km s^{-1}) allowing for the detection of both strong and weak CIV absorbsers. Our survey spans absorption redshifts from $0.18 < z < 2.57$, allowing for characterization of the evolution of the distribution of these absorbers across cosmic time. Using our own detection and analysis software, we are able to accurately characterize the equivalent width detection limit, absorption path length, and survey copmleteness to a level allowing for an accurate determination of dN/dZ, the equivalent width distribution function, the column density distribution function, and the total cosmic mass density of CIV absorbers. Our main findings are as follows:

1. Stuff
2. Things
3. more stuff and things

M.T.M. thanks the Australian Research Council for *Discovery Project* grant DP130100568 which supported this work. C.W.C. thanks the National Science Foun-

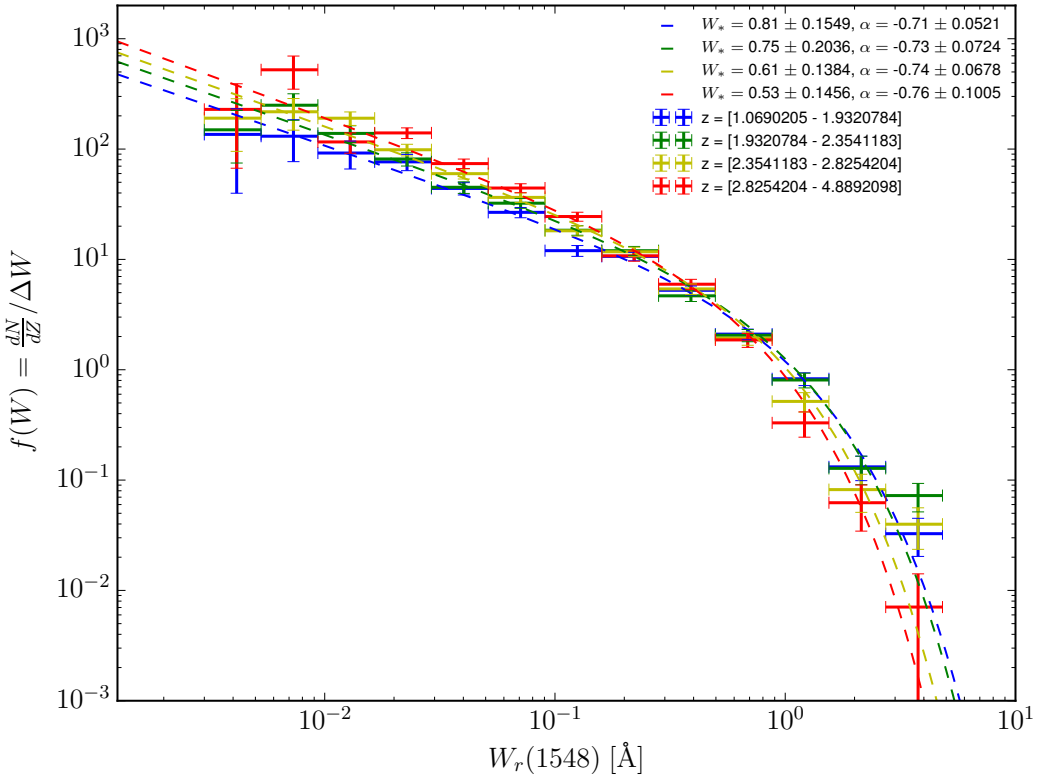

Figure 7. The equivalent width distribution of C IV absorbers, defined as the comoving line density ($\frac{dN}{dX}$) in each equivalent width bin divided by the bin width. We fit this distribution with a Schechter function, capturing the self-similar power law behavior of the distribution before the exponential cutoff limiting the size of C IV absorbers.

dation for the grant AST-1517816, which partially supported this work.

REFERENCES

Haardt, F., & Madau, P. 2012, ApJ, 746, 125

O'Meara, J. M., Lehner, N., Howk, J. C., et al. 2015, AJ, 150, 111

Quiret, S., Péroux, C., Zafar, T., et al. 2016, MNRAS

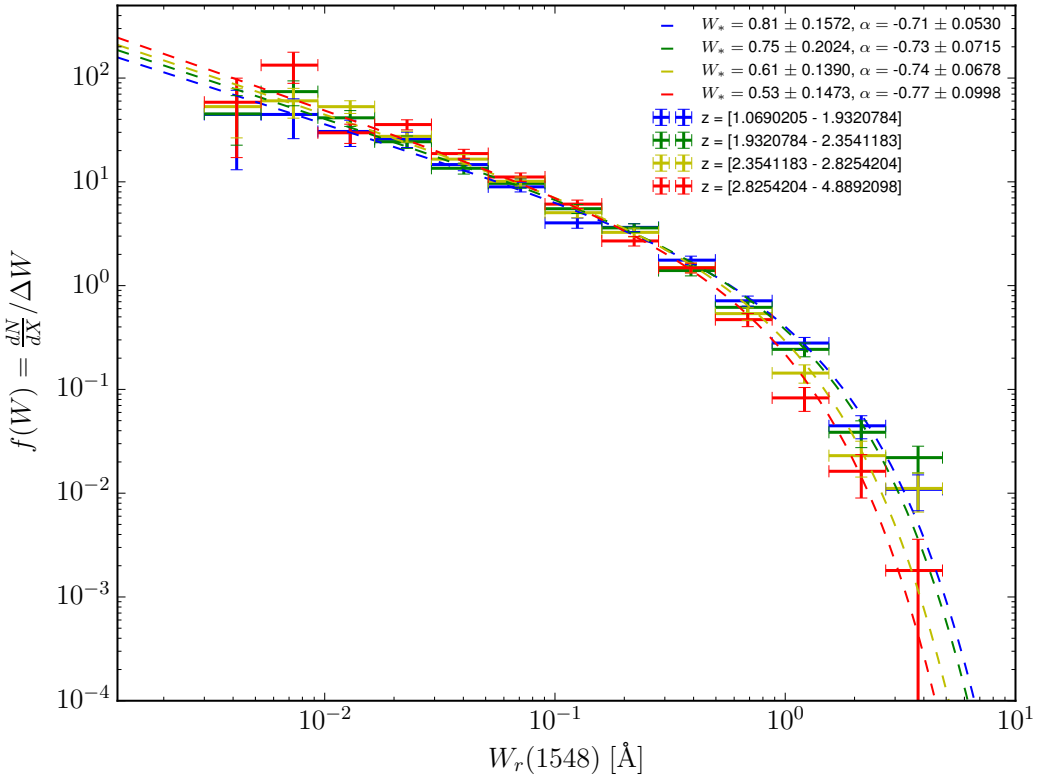

Figure 8. The equivalent width distribution of C IV absorbers, defined as the comoving line density ($\frac{dN}{dX}$) in each equivalent width bin divided by the bin width. We fit this distribution with a Schechter function, capturing the self-similar power law behavior of the distribution before the exponential cutoff limiting the size of C IV absorbers.

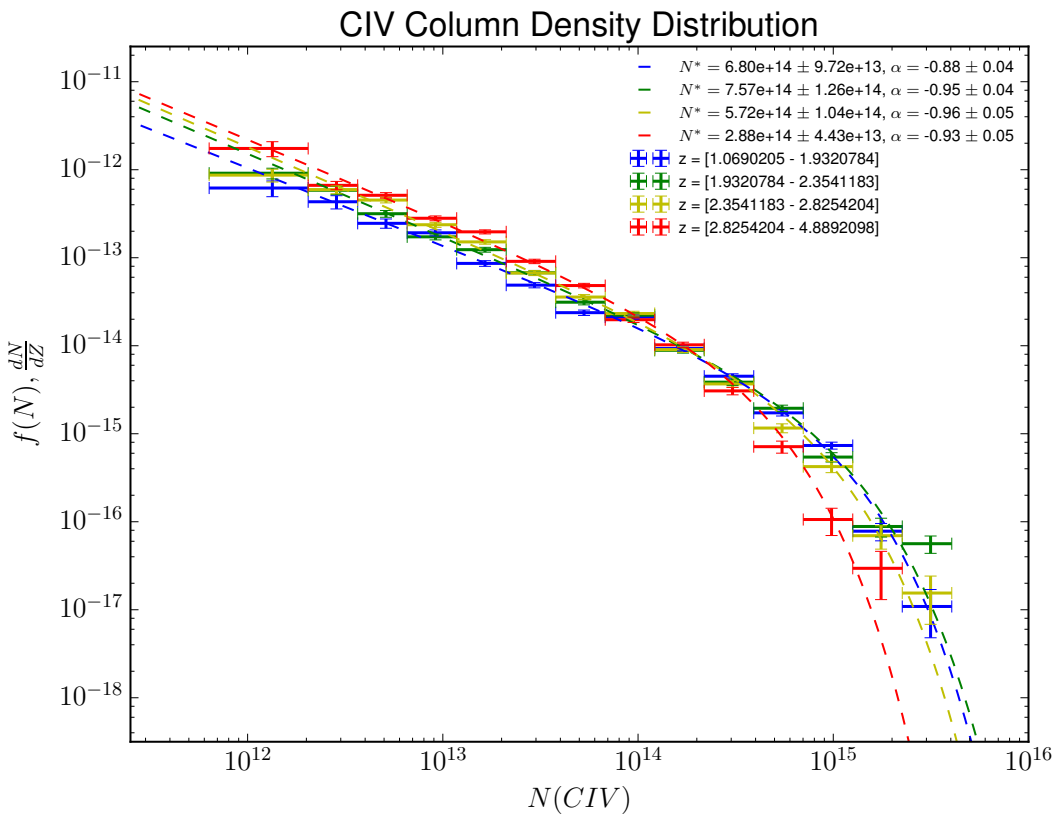

Figure 9. The column density distribution of CIV absorbers, defined as the comoving line density in each column density bin divided by the bin width. We fit this distribution with a Schechter function.

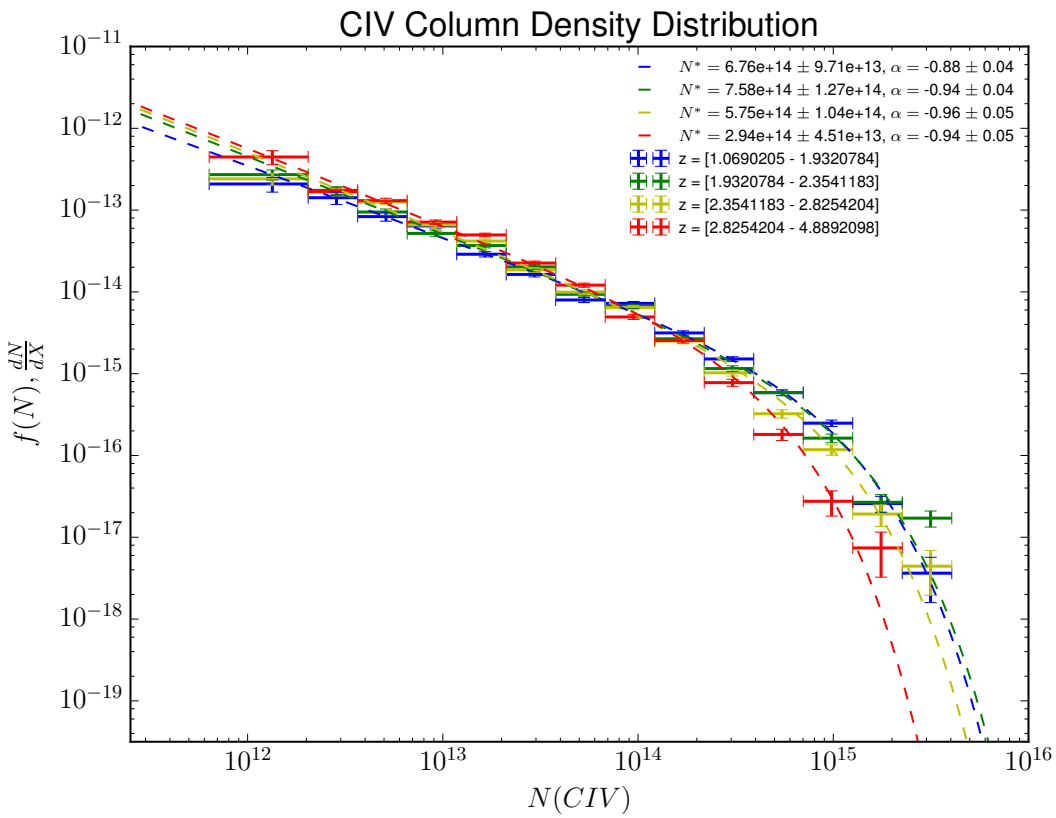

Figure 10. The column density distribution of CIV absorbers, defined as the comoving line density in each column density bin divided by the bin width. We fit this distribution with a Schechter function.

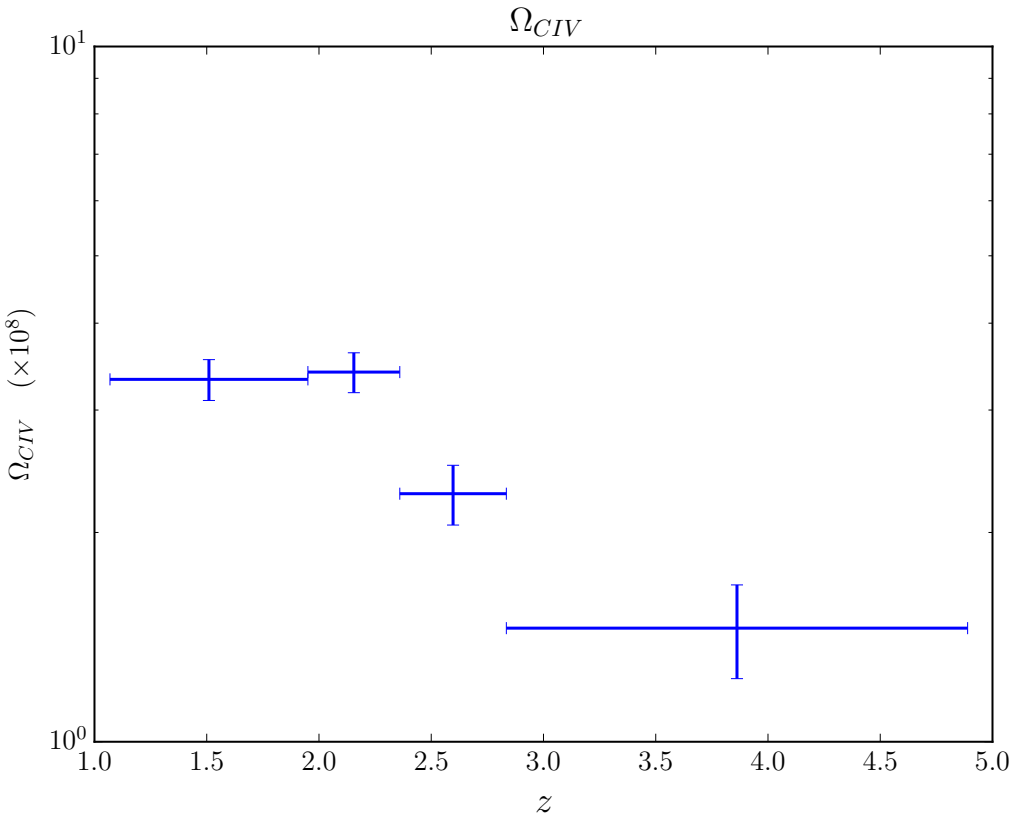

Figure 11. $\Omega_{\rm C\,IV}$ as a function of redshift. The cosmic mass density of C IV stays roughly flat near a value of 1×10^{-9}, with a potential increase from $z = 0.1$ to $z = 2.5$.